VOL. 11, NO. 18, SEPTEMBER 2016 ISSN 1819-6608
ARPN Journal of Engineering and Applied Sciences

www.arpnjournals.com

ELECTRONIC PROPERTIES CONTROL OF SUPER GROWTH SWCNT WITH METHYLENE BLUE DYE ADSORPTION

Fitri Khoerunnisa[1], Toshihiko Fujimori[2], Hendrawan[1] and Katsumi Kaneko[2]
[1]Department of Chemistry, Indonesia University of Education, Bandung, Indonesia
[2]Research Center for Energy and Environmental Sciences, Shinshu University, Japan
E-Mail: fitri.khoerunnisa@gmail.com

ABSTRACT

We demonstrated the facile and simple route to modify electronic properties of SG(SWCNT) with MB dyes through liquid phase adsorption. The adsorption of MB molecules into the tubes was proved by the notable decrease of X-ray diffraction intensity, depression of the N_2 and H_2 adsorption uptake at 77 K, and disordered bundle structure of SWCNT obtained from SEM image. The modification of electronic properties of SG(SWCNT) with MB adsorption was remarkably clarified by optical absorption spectra as well as the increase of electrical conductivity owing to the transition in metallic and/or semiconducting nanotubes through the molecular charge transfer interaction between pairs of van Hove singularities. Controlling electronic properties of SWCNT are supposed to be essential for its application in optoelectronic devices.

Keywords: electronic properties, super growth SWCNT, methylene blue, adsorption.

INTRODUCTION

The unique properties of SWCNT such as their high aspect ratio, high carrier mobility, and maximum current densities, make them an attractive component for nanometer scale optoelectronic devices (Tasis *et al*., 2003), (Burghards and Balasubramanian, 2005). Furthermore, SWCNT have a tendency to form a bundle structure offering interstitial and intratube nanopores surrounded by positively and negatively curved single-wall carbons, respectively. Both kinds of bundled SWCNT nanopores have a deep interaction potential well for various molecules and ions. The super-growth (SG) SWCNT most recently reported by Hata *et al*. which is a vertically growth of SWCNT produced by water-assisted chemical vapor deposition (CVD) offers high purity, selectivity, uniformity, and specific surface area. The average diameter obtained from TEM measurement is about 2.85 nm (Hata *et al*., 2004), (Fubata *et al*., 2006). The SG(SWCNT) seem to be different with other SWCNT samples because it consist a less dense bundle structure that can be regarded as nearly free-standing assembly of the nanotubes and offering strong adsorption field. The presence of these defects and the loosely packed assembly structure may play an important role in the high selectivity on the super-growth SWCNT assembly and thereby promising for adsorption study (Nishino *et al*., 2007).

The adjustment of SWCNT properties is essential to improve their performance, developing intriguing applications. Several approaches to modify the properties of SWCNT have been proposed (Georgakilas *et al*., 2008), (Guldi *et al*., 2005). The modification can be achieved by combining a SWCNT with an appropriate molecule. The selective interaction between chemical species and carbon nanotubes can lead to an efficient chirality-controlled separation of SWCNT (Campidelli *et al*., 2007), (Lurlo *et al*., 2008), (Varghese *et al*., 2009). In particular, functionalization of SWCNT allows one to enhance their electronic properties and is therefore extremely important for their applications. A more attractive functionalization strategy is to adsorb organic molecules into the SWCNT without breaking the chemical bonds. SWCNT are unique solids for interface chemistry because all carbon atoms of SWCNT are faced to interfaces of positive and negative curvatures (Fujimori *et al*., 2015). Typically, carbon nanotubes acquire a framework structure with sp^2 carbon. The sidewall of nanotubes is highly hydrophobic and exhibit the extended π-stacking (Debnath *et al*., 2010). Such properties permit them to interact with aromatic molecules possessing the π-conjugated structure. Gotovac *et al*. found the notable effect of nanoscale curvature of single wall carbon nanotubes on adsorption of polycyclic aromatic hydrocarbon (Gotovac *et al*., 2007). Furthermore, the π-electron coupling between aromatic molecules and carbon nanotubes can modulate their electronic and transport properties. On the other hand, the molecular structure of methylene blue (MB) is close to polycyclic aromatic hydrocarbon with π-conjugated nature, being a candidate for specific interaction with SWCNT. The electronic functionalization of carbon nanotubes with MB dye through site-selective physical adsorption using non-covalent bonding is expected to extend their performance (Khoerunnisa *et al*., 2012). The physisorbed MB molecules embedded in the internal tube spaces are predicted can tune the electronic structure of SWCNT regardless of a geometrical difficulty in the contact between the planar molecule and convex surface.

METHODOLOGY

Adsorption of MB dyes into super growth SWCNT

A cationic dye, methylene blue (MB) has molecular formula $C_{16}H_{18}N_3SCl.3H_2O$ and molecular weight of 373.90 g mol^{-1}. The methylene blue solution was dissolved in ethanol to provide different of MB concentration up to 60 mg L^{-1}. Prior to the adsorption experiment, the SG(SWCNT) was oxidized under a mixed nitrogen–oxygen gas at 750 K for removing the

amorphous carbons as well as their caps. The open-end caps structure both of SWCNT is favorable for molecular adsorption. Adsorption of MB solution on SG(SWCNT) was carried out at 298 K. The SWCNT of 1 mg was dispersed ultrasonically in MB solution over concentration range of 0.2 to 60 mg L^{-1} for adsorption measurement. The dispersion of SWCNT samples were filtered with a Millipore porous filter (0.45 µm) and washed by ethanol to remove any non-adsorbed MB molecules. The adsorption isotherm of MB on SG(SWCNT) was determined by measurement of the concentration change of MB solution using the maximum absorbance at 660 nm with an aid of UV-NIR spectroscopy (JASCO V-670). The MB-SG(SWCNT) samples were dried before characterization.

Characterization of MB-adsorbed SWCNT

Infrared spectra over range of 1000-4000 cm^{-1} were obtained by placing the sample on the KBr plate with the aid of FTIR spectrometer (JASCO; FT/IR-410). Each spectrum was 40 scans collected at a resolution of 2 cm^{-1}. Thermal gravimetric analysis was performed on TG/DTA apparatus (SHIMADZU; DTG-60AH) in the N_2 gas. The gas flow and heating rates were 300 mL min^{-1} and 5 K min^{-1}, respectively. The nanoporosity change of SWCNT with MB adsorption was examined with N_2 and H_2 adsorption at 77 K using a volumetric apparatus (Quantachrome) after preheating at 423 K and 10^{-4} Pa for 2 h. The pore structure parameters were obtained by subtracting pore effect (SPE) method (Kaneko and Ishii, 1992). X-ray diffraction patterns were measured at room temperature using the synchrotron X-ray with a radiation wavelength of 0.09976 nm at the Super Photon Ring (Spring-8, Hyogo, Japan); the scanning electron microscopy (SEM) images were taken by means of field emission scanning electron microscope (FE-SEM; JEOL, JSM-6330F). The Raman spectrometer applied (JASCO; NRS-3100) was equipped with a YAG laser (power 1.5 mW, wavelength 532 nm). Samples were exposed for 3 min with triple accumulations and spectra were taken at three different places on the surface of each sample for better reproducibility. The fabrication of SWCNT and MB-adsorbed SWCNT films were carried out by spray-coating method for optical absorption measurement, where the SWCNT and MB-adsorbed SWCNT dispersions were coated on polyethylene terephthalate (PET) substrate. The optical absorption spectra were collected using a UV-VIS-NIR spectrometer (JASCO; V-670). The DC-electrical conductivity of thin films was measured using four probes method.

RESULTS AND DISCUSSIONS

The adsorption isotherms of MB on SG(SWCNT) at 298 K is Langmuirian (Figure-1), indicating highly site-selective adsorption. The MB adsorption is almost saturated around 15 mg L^{-1} of MB equilibrium concentration on SG(SWCNT), supporting the site-selective-adsorption of MB-SG(SWCNT). The SG(SWCNT) shows the higher saturated adsorption amount and lower coverage of MB with the coverage of 0.10, indicates the fractional filling. The surface coverage was evaluated with the molecular complex model (Song *et al*., 2006). The treated SG–SWCNT having MB molecules of maximum filling were characterized after drying.

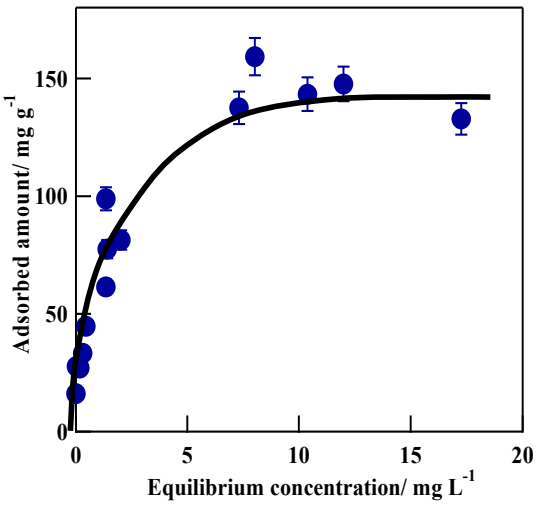

Figure-1. Adsorption isotherm of MB on SG (SWCNT) at 298 K.

The SEM image of SG(SWCNT) demonstrates the irregular assembly structures of nanotubes which are attributed to the presence of geometrical defects (Figure-2). The MB adsorption significantly causes the separation of assembly nanotubes of SG(SWCNT) due to the defect-induced adsorption field between the tube comprising and assembly.

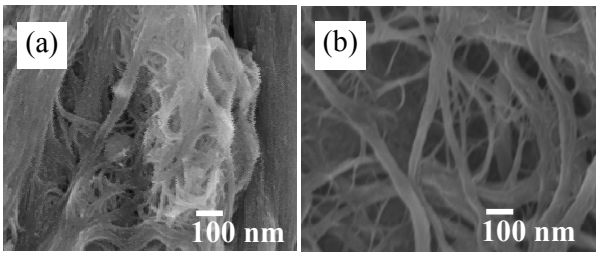

Figure-2. The SEM images of (a) SG(SWCNT) and (b) MB-SG(SWCNT).

The X-ray diffraction pattern of SG(SWCNT) (Figure-3) shows the broad peak with higher intensity at scattering factor of 1.51 $Å^{-1}$ relates to the reflection from the graphite lattice plane of 0 0 2 peak, corresponding to the spacing between planes in the atomic lattice distance of 0.41 nm. Two peaks at 3.02 and 5.08 $Å^{-1}$ are assigned to the reflection of graphite lattice planes of 1 0 and 1 1 peak, respectively. MB adsorption slightly changes the peak position and width, and decreases the peaks intensity, suggesting that MB molecules are not adsorbed in the interstitial spaces of nanotubes but predominantly exists inside nanotubes.

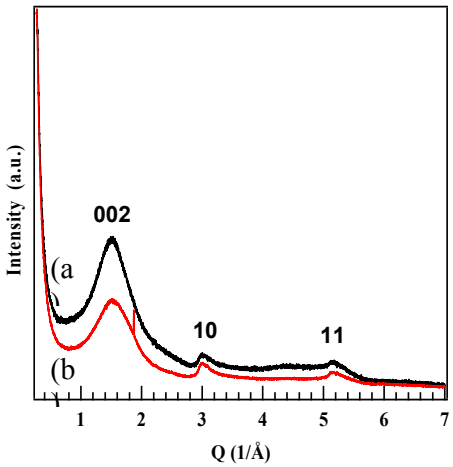

Figure-3. The X-ray diffraction patterns of (a) SG(SWCNT) and (b) MB-SG(SWCNT).

MB adsorption on SG(SWCNT) should contribute new functionalities that can be elucidated from FTIR spectra which provide the important information about adsorbed state of MB molecules on SWCNT. Figure-4 show the FTIR spectra of SG(SWCNT) that indicating the typical vibration modes of carbon nanotubes samples such as the peak at around 3400, 2920, 1600, 1380 and 1100 cm^{-1} corresponding to the stretching vibration modes of O-H, C-H of methylene group, C=C of benzene ring, C-H of alkanes and oxygen related functional groups, respectively. Since the MB molecules are predominantly adsorbed in the internal tube spaces of SWCNT, the adsorbed MB will strongly bound with the internal tube walls, results in the strong effect of molecular motion in the internal tubes spaces, leading to the shrinking diameter of nanotubes.

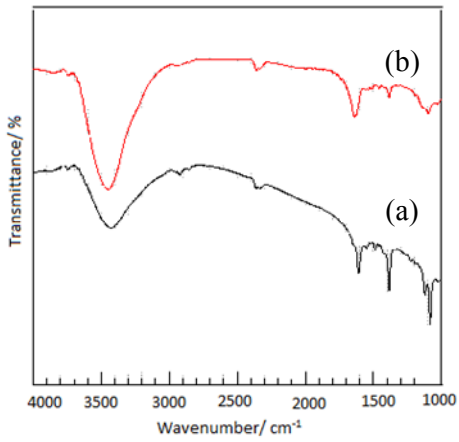

Figure-4. FTIR spectra of (a) SG(SWCNT) and (b) MB-SG(SWCNT).

The MB adsorption treatment on SG(SWCNT) induces remarkable the higher frequency shifts especially at 3448, 1636 and 1120 cm^{-1} corresponding to the stretching vibration modes of secondary amine, C=C of benzene ring and oxygen related functional group, respectively. Accordingly, it can be suggested that interaction of MB molecules with carbon nanotubes predominantly involves the aromatic backbone and secondary amine moieties, supporting the π-π interaction.

Thermal gravimetric (TG) analysis provides a quantitative estimation of the thermal stability of SWCNT as well as the amount of adsorbed MB molecules on SG(SWCNT). Figure 5 show the TG profile of SG(SWCNT) indicating the high purity sample. The significant weight loss observed in the temperature range below 700 K on both sample corresponds to decomposition of MB moieties adsorbed in SWCNT owing to its thermally labile nature. The total weight loss of MB-SG(SWCNT) is due to higher MB adsorption amount measured from adsorption isotherms. The weight loss verifies the MB adsorption on SG(SWCNT).

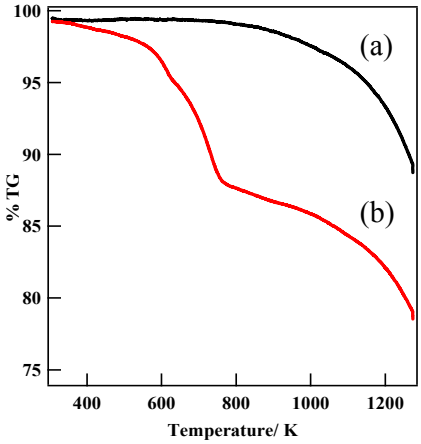

Figure-5. Thermal gravimetric profiles of (a) SG(SWCNT) and (b) MB-SG(SWCNT).

The porosity change of SG(SWCNT) on MB adsorption was evaluated by nitrogen adsorption at 77 K. The adsorption isotherm of nitrogen on SG(SWCNT) are of IUPAC type II, as shown in Figure 6. The adsorption of nitrogen at higher *P/Po* derives from multilayer adsorption on the external surface of the bundles and in larger mesopores and macropores due to the interbundle gaps. The MB adsorption treatment remarkably decreases the nitrogen adsorption amount at the holes pressure ranges and the adsorption isotherm of MB-adsorbed SWCNT just shifts downwards, indicating that MB molecules are preferentially adsorbed in the micropores as strongest adsorption sites in the SWCNT.

The pore structure parameters of SG(SWCNT) before and after MB adsorption were evaluated with subtracting pore effect (SPE) method using α_s plots of nitrogen adsorption at 77 K (Kaneko and Ishii, 1992) which are summarized in the Table-1.

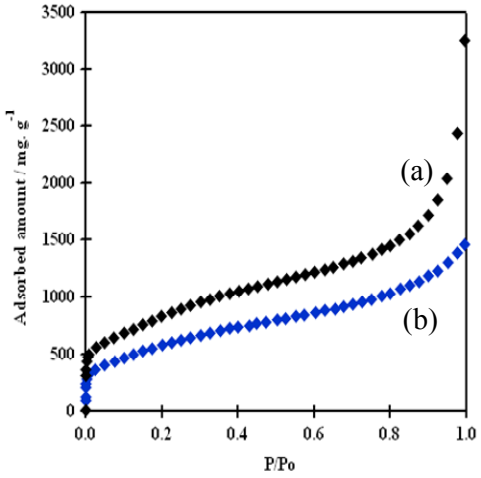

Figure-6. Nitrogen adsorption isotherms at 77 K on (a) SG(SWCNT) and (b) MB-SG(SWCNT).

The large total surface area of SG(SWCNT) is due to loosely-assembled structure and the tubes bundle does not tightly compact each other thus most the external surface is exposed to nitrogen molecules. The MB adsorption treatment notably decreases the surface area as well as nanopore volume of both SWCNT. The mesopore volume was obtained by subtracting the micropore volume from the total pore volume. The X-ray diffraction examination showed that MB molecules cannot be observed in the interstitial space of SWCNT thus MB molecules should be adsorbed in the internal tube spaces due to diffraction intensity decrease. The possible excluded volume of MB molecules adsorbed on SG (SWCNT) corresponding to 0.10 filling is evacuated to 0.17 mL g^{-1}.

Adsorption of supercritical H_2 at 77 K also supports selective filling of micropores with MB molecules, because supercritical H_2 can be preferentially adsorbed only in the smaller micropores having relatively strong interaction potential with an H_2 molecule. Figure 7 shows a marked drop in H_2 adsorption with the MB treatment. The adsorption amount of H_2 on the MB-SG(SWCNT) is about 50%, being the intensive depression of H_2 adsorption compared with that of N_2 adsorption. Thus, N_2 and H_2 adsorption supports that MB molecules are adsorbed in the internal tube spaces of the SG(SWCNT) bundles.

Using the assumption that the density of H_2 adsorbed in nanopores equals to the bulk density (0.078 g mL^{-1}) at 20 K the adsorption depression due to the MB adsorption on SG(SWCNT) of 16 mg g^{-1} corresponds to 0.21 mL g^{-1}, being close to that of N_2 adsorption. This is also supported by the isosteric heat of N_2 adsorption obtained from the Dubinin-Radushkevich (DR) plot (Noguchi *et al*., 2010). The DR equation has been widely used to describe the supercritical gas adsorption in nanopores as shown in equation 1.

$$W/W_0 = exp[-(A/E)^2], \quad A = RT\ ln(P_0/P), \quad E = \beta E_0 \qquad (1)$$

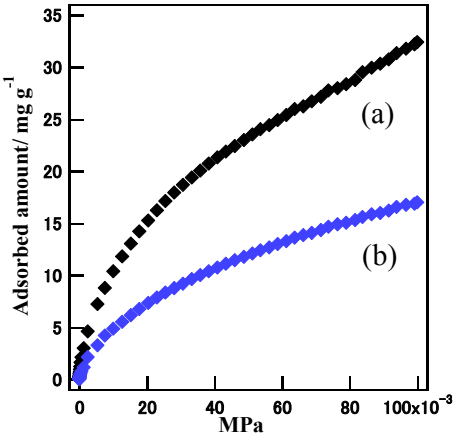

Figure-7. Hydrogen adsorption isotherms at 77 K on (a) SG(SWCNT) and (b) MB-SG(SWCNT).

where W is the amount of adsorption at P/P_0, W_0 is the limiting amount of adsorption, which generally corresponds to the nanopore volume, E_0 and β are characteristic adsorption energy and affinity coefficient, respectively. The βE_0 value can lead to the isosteric heat of adsorption, $q_{st,1/e}$, at fractional filling of $1/e$ using enthalpy of vaporation (ΔHv) at the boiling point through the equation 2.

$$q_{st,1/e} = \Delta H_v + \beta E_0 \qquad (2)$$

The DR plots were linear in the low pressure region where the $q_{st,1/e}$ value for the SG(SWCNT) and MB-SG(SWCNT) are 11.4 and 10.8 kJ mol^{-1}, respectively. The smaller $q_{st,1/e}$ value of the MB-adsorbed SWCNT suggests the relative increase of the wider pores due to the occupation of the narrower micropores by pre-adsorbed MB. It is well-known that bundled SWCNT provides the adsorption sites. Among them, the interstitial site and internal space have the higher potential adsorption, owing to the narrower spaces. Since the interstitial site is not accessible for MB molecules owing to the smaller size than that of MB, the internal tubes space should easier to be filled by MB molecules than the interstitial sites due to the geometrical restriction of the interstitial sites for the MB molecules. When MB molecules are introduced inside tubes, it must interact with the internal tube wall of negative curvature. The MB molecules having a π-conjugated structures must give rise to charge transfer interaction with the aromatic backbone of nanotubes wall, results in the charges on the SWCNT walls. The charge on the SWCNT should partially unravel the bundle structure.

A detailed analysis of the radial breathing mode (RBM) can provide the additional information about interaction of MB molecules with SWCNT particularly, to determine SWCNT diameters. The RBM frequency of SWCNT is actually sensitive to influence by chemical and

physical factors as well as tube diameters (Voggu *et al*., 2008). The chemical factor is chemical doping or functionalization by electron acceptor or donor dopants (upshift or downshift due to charge transfer between dopant and SWCNT).

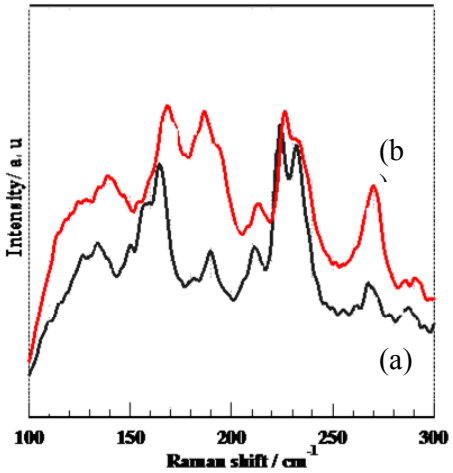

Figure-8. The radial breathing modes of (a) SG(SWCNT) and (b) MB-SG(SWCNT).

The most representative physical factors are bundle size, pressure, and temperature effects, which are related mainly to van der Walls forces and strength of carbon-carbon force constant of SWCNT (Fujimori *et al*., 2015). The relationship between RBM frequency and diameter of SWCNT can be expressed by equation 3.

$$\omega_r\,(cm^{-1}) = \frac{a}{d}\,(nm\,cm^{-1}) + b \qquad (3)$$

where *a* constant is 227 and *b* constant equals to zero (Noguchi *et al*., 2010)

Table-1. Porosity parameter of SG(SWCNT) and MB-SG(SWCNT).

Parameter	SG (SWCNT)	MB-SG (SWCNT)
S_{BET} / m^2g^{-1}	2280	1300
Mesopore volume / mL. g^{-1}	2.10	1.42
Micropore volume / mL. g^{-1}	0.85	0.55

The SG(SWCNT) shows the multipeaks distribution of the tube diameter range from 0.8 to 1.4 nm (Figure 8). The MB adsorption shifts the RBM peak of SG(SWCNT) to the higher frequency results in the smaller diameter. The diameter reduction should associate with the encapsulation of MB molecules in the internal tubes where the aromatic backbone and the functional entities of MB molecules should strongly interact with the nanotubes wall. Since the molecular structure of MB allows the delocalization of electronic charge and promoting the extended π-conjugated system of SWCNT network, the higher frequency shift of RBM corresponds to the π-π interaction between SWCNT and MB molecules, creating a "mode hardening effect"(Gotovac *et al*., 2007).

It is well recognized that the optical response of SWCNT is dominated by transition between pairs of van Hove singularities in the electron density of state (Maeda *et al*., 2005), (Shin *et al*., 2008). The electronic structure change of SWCNT with MB adsorption can be probed with optical absorption spectroscopy. The SG(SWCNT) (Figure 9) exhibits the weak optical band at around 1700 and 1900 nm corresponds to the first semiconducting transition (S_{11}) nanotubes, indicating the high purity of SWCNT.

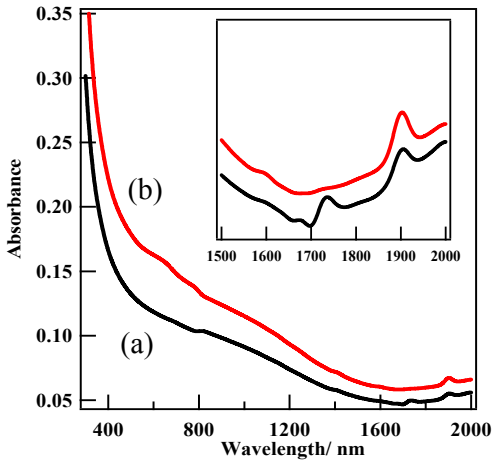

Figure-9. Optical absorption spectra (OAS) of (a) SG (SWCNT) and (b) MB-SG(SWCNT). Inset figure is the magnified OAS at higher wavelength.

The MB encapsulation in SG(SWCNT) changes their electronic structure where the one of the S_{11} peak transition disappears and new broad peak with the weak intensity at around 600 nm can be observed, suggesting the selective destruction of semiconducting nanotubes and give rise to metallic nanotubes (Kuzmany *et al*., 2004). This result reveals the charge transfer interaction between SG-SWCNT and MB molecules.

Table-2. Electrical conductivity of SG (SWCNT) at different MB coverage.

MB coverage (θ)	σ / S.m
0	52.68
0.06	66.08
0.08	84.16

The electrical conductivity measurement supports the evidence of molecular charge transfer (Table-2). The MB adsorption increases the electrical conductivity of SG(SWCNT), suggesting the molecular charge transfer

interaction between MB molecules and SWCNT. Thus, MB adsorption efficiently modify electronic properties of SG(SWCNT).

CONCLUSIONS

We have shown that adsorption of MB on SWCNT in liquid phase is believed to be an efficient route for electronic property control of SWCNT. The adsorption of MB inside the tubes was verified by the remarkable decrease of X-ray diffraction intensity, depression of the N_2 and H_2 adsorption uptake at 77 K, and disordered bundle structure of SWCNT obtained from SEM image. The RBM and optical absorption spectra clarified the modification of electronic structure of SWCNT with MB adsorption owing to the transition in metallic and/or semiconducting nanotubes through the molecular charge transfer interaction between pairs of van Hove singularities as strongly verified by transition of optical absorption spectra and the increase of electrical conductivity. The dye modified SWCNT system should be crusial for processing of SWCNT in various applications of optoelectronic devices.

ACKNOWLEDGEMENT

The financial and technical supports provided by Ministry of Research and Technology, KEMENRISTEK Indonesia, under Fundamental and International Collaborative Grants 2015. We thank to Prof. K. Hata for kindly providing the SG(SWCNT). We also appreciate to Department of Chemistry, UPI for the travel grant.

REFERENCES

Burghard, M., Balasubramanian, K. 2005. Chemically Functionalized Carbon Nanotubes. Small, 1(2), pp. 180-192.

Campidelli, S., Meneghetti, M., Prato, M. 2007. Separation of Metallic and Semiconducting Single-Walled Carbon Nanotubes via Covalent Functionalization. Small, 3(10), pp.1672-1676.

Debnath, S., Cheng, Q., Hedderman, T.G., Bryne, H.J. 2010. Comparative Study of the Interaction of Different Polycyclic Aromatic Hydrocarbons on Different Types of Single-Walled Carbon Nanotubes. J. Phys. Chem. C, 114(18), pp. 8167-8175.

Fubata, D.N., Hata, K., Namai, T., Yamada, T., Mizuno, K., Hayamizu, Y., Yumura, M., Iijima, S. 2006. 84% Catalyst Activity of Water-Assisted Growth of Single Walled Carbon Nanotube Forest Characterization by a Statistical and Macroscopic Approach. J. Phys. Chem. B, 110(15), pp. 8035-8038.

Fujimori, T., Khoerunnisa, F., Ohba, T., Gotovac, S., Tanaka, H., Kaneko, K. 2015. Function of Conjugated π-Electronic Carbon Walled Nanospaces Tuned by Molecular Tiling, Electronic Processes in Organic Electronics. Springer Series in Materials Science, 209, pp. 351-378.

Georgakilas, V., Bourlinos, A., Gournis, D., Tsoufis, T., Trapalis, C., Alonso, A., Prato, M. 2008. Multipurpose Organically Modified Carbon Nanotubes: From Functionalization to Nanotube Composites. J. Am. Chem. Soc., 130(27), pp. 8733-8740.

Gotovac, S., Honda, H., Hattori, Y., Takahashi, K., Kanoh, H., Kaneko, K. 2007. Effect of Nanoscale Curvature of Single-Walled Carbon Nanotubes on Adsorption of Polycyclic Aromatic Hydrocarbons. Nano Lett., 7(3), pp. 583-587.

Guldi, D.M., Rahman, G.M.A., Zerbetto, F., Prato, M. 2005. Carbon Nanotubes in Electron Donor-Acceptor Nanocomposites. Acc. Chem. Res., 38(11), pp. 871-878.

Hata, K., Fubata, D.N., Mizuno, K., Namai, T., Yumura, M., Iijima, S. 2004. Water-Assisted Highly Efficient Synthesis of Impurity-Free Single-Walled Carbon Nanotubes. Science, 306, pp. 1362-1364.

Khoerunnisa, F., Fujimori, T., Itoh, T., Urita, K., Hayashi, T., Kanoh, H., Ohba, T., Hong, S. Y., Choi, Y. C., Santosa, S. J., Endo, M., Katsumi, K. 2012. Enhanced CO_2 Adsorptivity of Partially Charged Single Walled Carbon Nanotubes by Methylene Blue Encapsulation. J. Phys. Chem. C, 111(20), pp. 11216-11222.

Kaneko, K., Ishii, C. 1992. Superhigh Surface Area Determination of Microporous Solids. Colloids Surfaces 67, pp. 203-212.

Kuzmany, H., Kukovecz, A., Simon, F., Holzweber, M., Kramberger, C.H., Pichler, T. 2004. Functionalization of Carbon Nanotubes, Synthetic Metal, 141(1-2), pp. 113-122.

Lurlo, M., Paolucci, D., Marcaccio, M., Paolucci, F. 2008. Electron Transfer in Pristine and Functionalised Single-Walled Carbon Nanotubes, Chem. Commun., pp. 4867-4874.

Maeda, Y., Kimura, S., Kanda, M., Hirashima, Y., Hagesawa, T., Wakahara, T., Lian, Y., Nakahodo, T., Tsuchiya, T., Akasaka, T., Lu, J., Zhang, X., Gao, Z. Yu, Y., Nagase, Y. S., Kazaoui, S., Minami, S., Shimizu, T., Tokumoto, T., Saito, R. 2005. Large-Scale Separation of Metallic and Semiconducting Single-Walled Carbon Nanotubes, J. Am. Chem. Soc. 127(29), pp. 10287-10290.

Nishino, H., Yasuda, S., Namai, T., Fubata, D.N., Yamada, T., Yumura, M., Iijima, S., Hata, K. 2007. Water-Asissted Highly Efficient Synthesis of Single-Walled Carbon Nanotubes Forests from Colloidal Nanoparticle Catalyst, J. Phys. Chem. C. 111(48), pp. 17961-17965.

Noguchi, D., Tanaka, H., Fujimori, T., Kagita, H., Hattori, Y., Honda, H., Urita, K., Utsumi, S., Wang, Z. M., Ohba, T, Kanoh, H., Hata, K., Kaneko, K. 2010. Selective D_2 Adsorption Enhanced by the Quantum Sieving Effect on Entangled Single-Wall Carbon Nanotubes, J. Phys. Condens. Mater., 22(33) pp. 334207

Shin, H.J., Kim, S.M., Yoon, S.M., Benayad, A., Kim, K.K., Kim, S.J., Park, H. K., Choi, J.-Y., Lee, Y.H. 2008. Tailoring Electronic Structures of Carbon Nanotubes by Solvent with Electron-Donating and -Withdrawing Groups J. Am. Chem. Soc., 130(6), pp. 2062-2066.

Song, L., Miyamoto, J.-L., Kanoh, H., Nakahigashi, Y., Kaneko, K. 2006. Enhancement of the Methylene blue Adsorption Rate for Ultramicroporous Carbon Fiber by Addition of Mesopores, Carbon, 44(10), pp.1884-1890.

Tasis, D., Tagmatarchis, N., Georgakilas, V., Prato, M. 2003. Soluble Carbon Nanotubes, Chem. Eur. J., 9, pp. 4000-4008.

Varghese, N., Ghosh, A., Voggu, R., Ghosh, S., Rao, C.N.R. 2009. Selectivity in the Interaction of Electron Donor and Acceptor Molecules with Graphene and Single-Walled Carbon Nanotubes, J. Phys. Chem. C, 113(39) pp. 16855-16859.

Voggu, R., Rout, C.S., Franklin, A.D., Fisher, T.S., Rao, C.N.R. 2008. Extraordinary Sensitivity of the Electronic Structure and Properties of Single-Walled Carbon Nanotubes to Molecular Charge-Transfer, J. Phys. Chem. C, 112(34), pp. 13053-13056.